


Article

Design of Mega-Constellations for Global Uniform Coverage with Inter-Satellite Links

Lu Jia , Yasheng Zhang *, Jinlong Yu and Xuan Wang

Department of Aerospace Science and Technology, Space Engineering University, Beijing 101416, China; 18510793099@163.com (L.J.); yunudt@126.com (J.Y.); wx1449282350@stu.xjtu.edu.cn (X.W.)

* Correspondence: zhangyspublic@163.com

Abstract: Constellation configuration design is a prerequisite and critical step in the construction of a mega-constellation system in low Earth orbit. However, the huge number of satellites and the intricate changes in relative positions among them make the configuration design the most challenging part. In this paper, we propose a configuration design scheme for mega-constellations considering collision-avoidance constraints with the objective of uniform global coverage. In this design scheme, the constellation is made up of multiple Walker constellations with the same orbital altitude and different orbital inclination. Moreover, the analytical expression for the minimum distance between any two satellites in the same orbital altitude is derived, and the constellation internal collision-avoidance constraint is established accordingly. Finally, a permanent inter-satellite link design scheme without dynamic reconstruction is presented based on the mega-constellation configuration. Simulation results show that the mega-constellation design scheme introduced in this paper can achieve relatively uniform global coverage (its N Asset Coverage ranges from 18 to 25). The mixed Walker constellation is capable of providing a greater number of N Asset Coverage for most of the world than the Walker constellation of the same satellite order of magnitude. In addition, the inter-satellite link scheme designed in this paper can ensure continuous and stable communication between any satellite nodes.

Keywords: mega-constellations; collision avoidance; uniform global coverage; inter-satellite link; Walker constellation; sub-satellite point



Citation: Jia, L.; Zhang, Y.; Yu, J.; Wang, X. Design of Mega-Constellations for Global Uniform Coverage with Inter-Satellite Links. *Aerospace* **2022**, *9*, 234. <https://doi.org/10.3390/aerospace9050234>

Academic Editor: Pierre Rochus

Received: 11 March 2022

Accepted: 22 April 2022

Published: 24 April 2022

Publisher's Note: MDPI stays neutral with regard to jurisdictional claims in published maps and institutional affiliations.



Copyright: © 2022 by the authors. Licensee MDPI, Basel, Switzerland. This article is an open access article distributed under the terms and conditions of the Creative Commons Attribution (CC BY) license (<https://creativecommons.org/licenses/by/4.0/>).

1. Introduction

Recently, the rapid development of satellite manufacturing, reuse technology for launch vehicles, and multi-satellite launch technology have made the deployment of large-scale constellations (constellations containing hundreds or even thousands of satellites) in space a reality. Several companies have already proposed plans to construct mega-constellations in low earth orbit (LEO) [1]. The most popular ones, SpaceX and OneWeb, have already been put into practice. Among the various aspects of the mega-constellation system's construction, the constellation configuration design is a prerequisite to guarantee the regular operation of the constellation. It is also the key to ascertaining the constellation system's performance and application level. At the same time, the constellation configuration design is a complicated problem that requires integrated consideration of satellite orbit characteristics, temporal and spatial distribution, and overall system performance [2]. Furthermore, the rapid topological changes among LEO satellites and the increased collision risks [3] associated with the huge number of satellites increase the complexity of the constellation design. Therefore, the design of mega-constellations configuration is a significant and challenging study.

The traditional constellation design methods are mainly divided into two categories: One is the geometric analytical method [4], which combines space geometry and orbital dynamics to give the analytical form of the constellation configuration; additionally, the other

is the optimization design method [5], which applies intelligent optimization algorithms to find the configuration that makes the constellation performance optimal. The representative geometric analytical method is the Walker constellation, proposed by John Walker [6]. It can be accommodated to global coverage requirements. The properties of any satellite in the Walker constellation are the same. Afterward, various constellation configurations were derived based on the Walker constellation. Researchers such as Ballard [7], Lang [8], and Adams [9] contributed fruitful research results intending to use the minimum number of satellites to achieve global coverage. Rider [10] is concerned with the analysis of the coverage of latitudinal zones. The flower constellations (FCs) defined by Mortari [11] are similar to the Walker constellations. The FCs are suitable for the Earth observation missions due to their repeat ground track. Based on FCs theory, scholars later expanded the design possibilities and proposed constellation configurations such as 2D [12], 3D [13], and 4D [14] Lattice FCs, and then the Necklace FCs [15] and 2D [16] and 3D [17] Necklace FCs were developed. Arnas [18] presented a detailed simulation analysis for the application of 2D Necklace FCs to Earth observation missions. Huang [19] presented a systematic method for designing continuous global coverage Walker and Street-of-Coverage constellations by taking seven critical constellation properties as design criteria. The authors of [20] proposed a semi-analytical method in designing constellations to deal with a sequence of Earth revisit missions. The intelligent optimization design methods have significant strengths when the number of satellites is small or for regional coverage tasks. Han [21] solved the design of navigation constellations using the Multi-Objective Particle Swarm Optimization algorithm. Ma [22] designed a hybrid constellation using a genetic algorithm on an LEO-based navigation augmentation system. Wang [23] proposed a novel optimization method, the hybrid-resampling particle swarm optimization (HRPSO) algorithm, which improved the computational efficiency of constellation design.

The above research mainly focused on the design of traditional constellations with fewer than 100 satellites. However, there are only a few studies on the design of mega-constellations. Kak [24] proposed a large-scale constellation design optimization framework for CubeSats. It analyzed several framework cases applied to the Internet of Space Things (IoST). Ge [25] studied the constellation optimization problem for the LEO enhanced global navigation satellite system (LeGNSS) with 240 LEO satellites of orbital inclinations at 90° , 60° , and 35° selected. Ravishankar [26] introduced a hybrid communications architecture and a 5G unifying protocol architecture based on mega-constellations. This work balanced all aspects of system design for such large and complex systems. Based on the Starlink constellation, Khalife [27] proposed a framework to navigate LEO satellite signals with differential carrier phase measurements. Arnas [28] applied FCs theory to generate sets of LEO slots free from self-conjunctions. He also innovatively proposed the 4D Lattice FCs design method and applied it to the design of mega-constellations [14]. While the constellation is capable of deploying more satellites at the same orbital altitude than the Walker constellation, this comes at the cost of a non-uniform distribution of satellites, preventing the constellation from achieving sustained global coverage. In summary, more and more creative findings are emerging for mega-constellations. However, almost all studies are based on a Walker constellation to explore the application value of mega-constellations. Few have focused on the in-depth research of constellation configuration design.

The successful practice of the Walker constellations in GPS [29], Glonass [30], Iridium [31], and other space systems has proven its significant superiority in serving traditional space missions. However, when the number of satellites increased to the order of thousands, the serious unevenness of the Walker constellation's coverage along the latitude zones became prominent. Its sub-satellite points will show a trend of sparse distribution at low latitudes and extremely dense distribution at high latitudes [32]. This drawback not only causes the waste of space resources but more seriously, a large number of satellites accumulate over high latitudes, increasing the risk of collision between satellites and threatening the space security environment. Although this weakness can be mitigated by using a constellation configuration with multiple orbital layers mixed, it will significantly

increase the complexity of the inter-satellite links (ISLs) design, since two satellites between different orbital altitudes cannot communicate continuously. Thus, it is relevant to design a constellation configuration that can improve global coverage performance, consider collision avoidance, and be in the same orbital layer.

Establishing ISLs [33] within the mega-constellation provides many advantages, such as reduced communication delay, path loss, and inter-satellite data transmission independent of the ground systems [34]. The mega-constellation is a huge space-based information network platform. Each satellite node is not an independent individual but works in concert to pursue the maximum functionality of the overall system. Therefore, inter-satellite communication capability will become a necessary attribute for mega-constellations. It means that ISLs design will also be an integral part of the design of the mega-constellations.

Based on previous efforts, this paper is dedicated to studying the design of mega-constellations. We propose a mixed Walker constellation design method that achieves full-time domain and global uniform coverage. It considers the collision-avoidance problem within the constellation, and all satellites orbit at the same altitude. Based on this constellation configuration, we introduce an ISL design scheme that guarantees stable data transmission within the mega-constellation. Firstly, we define a metric that measures the distribution density of the sub-satellite points along the latitudinal zones. Using this metric as a benchmark, sub-constellations with different orbital inclinations are obtained in turn. Secondly, considering the collision-avoidance problem, the analytical expression for the minimum distance between any two near-circular orbiting satellites of the same orbital altitude is derived based on the orbital dynamics and spatial geometry. The orbital parameters of some satellites are adjusted in the mega-constellation until the minimum distance between any two satellites is greater than a safe distance. Thirdly, the ISL is established based on the principle that the maximum distance between two satellites in the constellation is minimized. An ISLs design scheme that avoids link reconstruction during the constellation operation is obtained, which ensures stable inter-satellite communication to a certain extent. Finally, the mixed Walker constellations theory introduced in this paper is applied to design a 5685-satellite mega-constellation using a circular orbit. The simulation analysis results verify its global uniform coverage as well as its ability to communicate continuously.

Summarized, the main contributions of this paper are as follows: First, while a constellation containing a large number of satellites can easily achieve global coverage, the mega-constellation designed in this paper can significantly improve the quality of global coverage. On top of satisfying global coverage, it not only provides more uniform coverage but also increases the number of N Asset Coverage over most of the globe. Second, we derive the minimum distance between any two satellites at the same altitude using a geometric approach, which is more tangible and comprehensible than the algebraic approach in [35]. Third, although the literature [36] also considers the continuous communication of ISLs when performing the constellation design, it only uses a constellation containing 44 satellites with the same orbital inclination for research. However, this paper studies the ISLs design method with higher complexity and more in line with the actual operation of mega-constellations.

The remainder of the paper is structured as follows. Section 2 presents the theory and methodology for establishing the mega-constellation design model. Section 3 provides a design model of the inter-satellite links for the mega-constellations. Section 4 develops the models in detail, and a corresponding numerical simulation is performed. Finally, conclusions are drawn.

2. Mega-Constellation Design Model

The distribution of satellites determines the coverage performance of the constellation [37], and the more uniformly the satellites are scattered across the celestial sphere, the better for rapid coverage over large areas. The most widely used Walker constellation covers all the longitudes uniformly with time but suffers from a significant problem of

uneven coverage on the latitude zones. This shortcoming will be even more pronounced when the number of satellites is large.

Aiming at designing a mega-constellation capable of achieving uniform global coverage of the ground, it is first necessary to define a metric that measures the density of the constellation's sub-satellite points over the latitudinal zones. Furthermore, the Walker constellation can be used as the basic unit of a mega-constellation, taking advantage of its symmetry and uniform coverage of all longitudes. In addition, the latitudinal coverage is restricted by the orbital inclination of the satellites within the constellation. A mixed Walker constellation configuration with multiple inclinations is required to provide balanced coverage of the various latitudinal zones.

The mega-constellation configuration design in this paper can be summarized as follows: Using the Walker constellation as the basic unit, the density of the sub-satellite points on the latitude zone is adopted as an indicator, and sub-constellations with different orbital inclinations are generated in successive iterations. At the same time, the initial orbital planes of the sub-constellations are evenly spaced on the equator to ensure that the sub-satellite points are sufficiently uniform in the longitudinal direction. We have acquired a preliminary constellation configuration up to this point. Then, the collision-avoidance constraint is established according to the relative position between satellites, and the orbit parameters of some satellites with high collision risk are adjusted. The final constellation configuration is derived.

2.1. Prerequisite Conditions for the Model

Before going into details, some prerequisite conditions need to be clarified to ensure the rationality of the model. The specific content is as follows:

- (1) In general, the relative distances of two satellites with different orbital altitudes vary continuously with time, which will eventually lead to the two satellites not satisfying the geometric visibility condition. In other words, a stable ISL cannot be established between satellites with different orbital altitudes. Therefore, to establish durable and stable ISLs within the mega-constellation system, all satellites are required to be at the same orbital altitude.
- (2) For LEO satellites, the non-spherical gravitational perturbation and atmospheric drag perturbation will have a noticeable impact on satellite orbit. In particular, the drift of the ascending node caused by the J_2 perturbation is significant. In the long run, the constant change in the relative drift of the ascending nodes between satellites with different inclinations will prevent the constellation from operating in an orderly manner according to the initial configuration. Though the effects of perturbation can be circumvented by placing satellites with different orbital inclinations at different orbital altitudes, the different orbital altitudes can bring trouble to the establishment of ISLs, as illustrated in (1). For heterogeneous constellations with satellites of the same orbital altitude and different orbital inclinations, the long-term impact of perturbation on the constellation configuration cannot be solved by the constellation configuration design. Therefore, this paper focuses on the configuration design of the mega-constellations with a two-body orbit model. The long-term maintenance of the constellation configuration will be studied in depth in the subsequent work.

2.2. Walker Constellation

The Walker constellation comprises a certain number of satellites with the same orbital inclination, semimajor axis, eccentricity, and argument of perigee (i, a, e, ω). Three integer parameters of the total number of satellites N , the number of orbital planes P , and the configuration number F determine the configuration of the Walker constellation. Using the

three parameters (N, P, F) , the mean anomaly M and the right ascension of the ascending node Ω of the j -th satellite on the i -th orbital plane can be obtained [38].

$$\begin{cases} \Omega_{ij} = \Omega_0 + \frac{2\pi}{P}(i - 1) \\ M_{ij} = M_0 + 2\pi \cdot \left[\frac{F}{N}(i - 1) + \frac{P}{N}(j - 1) \right] \end{cases} \quad (1)$$

where $i = 1, 2, \dots, P, j = 1, 2, \dots, N/P$, and the data range of F is $F \in [0, P - 1]$. Ω_0 and M_0 represent the datum values of the RAAN and the mean anomaly, respectively.

2.3. Ground Tracks

The position of the sub-satellite point on the Earth’s surface can be obtained by the coordinate system transformation. The coordinate transformation sequence is as follows: the perifocal reference frame \rightarrow earth-centered inertial frame (ECI) \rightarrow earth-centered, earth-fixed frame (ECEF) [39] \rightarrow spherical coordinate system [40]. The specific solution of the satellite’s ground trajectory is as follows.

The satellite’s mean anomaly at time t can be written as:

$$M = t \cdot \sqrt{\frac{\mu}{a^3}} \quad (2)$$

where $\mu = 3.986 \times 10^5 km^3/s^2$ is the Earth gravitational constant [41].

According to the Kepler equation, the relationship between the eccentric anomaly E and the mean anomaly M is expressed as:

$$M = E - e \sin E \quad (3)$$

E can be obtained effectively by combining Equations (2) and (3), adopting the Newton iteration method. Then, we can calculate the true anomaly f .

$$f = 2 \arctan \left(\tan \frac{E}{2} \cdot \sqrt{\frac{1+e}{1-e}} \right) \quad (4)$$

Eventually, the satellite’s position in the perifocal frame is written as:

$$\mathbf{r} = \frac{h^2}{\mu} \frac{1}{1 + e \cos f} \begin{bmatrix} \cos f \\ \sin f \\ 0 \end{bmatrix} \quad (5)$$

The classical Euler angle sequence $M_3[\omega] \cdot M_1[i] \cdot M_3[\Omega]$ can convert the satellite’s position from the perifocal frame to the ECI coordinate system. The transformation relationship is:

$$\mathbf{r}_{ECI} = \begin{bmatrix} \cos \omega \cdot \cos \Omega - \sin \omega \cdot \cos i \cdot \sin \Omega & \cos \omega \cdot \sin \Omega + \sin \omega \cdot \cos i \cdot \cos \Omega & \sin \omega \cdot \sin i \\ -\sin \omega \cdot \cos \Omega - \cos \omega \cdot \cos i \cdot \sin \Omega & -\sin \omega \cdot \sin \Omega + \cos \omega \cdot \cos i \cdot \cos \Omega & \cos \omega \cdot \sin i \\ \sin i \cdot \sin \Omega & -\sin i \cdot \cos \Omega & \cos i \end{bmatrix}^{-1} \cdot \mathbf{r} \quad (6)$$

The transformation from the ECI to the ECEF can be implemented by a rotation matrix $M_3[\theta] \cdot M_2[0] \cdot M_1[0]$, and θ is given by $\omega_e(t - t_0)$. The transformation is written as:

$$\mathbf{r}_{ECEF} = \begin{bmatrix} \cos \theta & \sin \theta & 0 \\ -\sin \theta & \cos \theta & 0 \\ 0 & 0 & 1 \end{bmatrix} \cdot \mathbf{r}_{ECI} \quad (7)$$

The longitude and latitude (α, δ) of the satellite’s projection on the Earth’s surface can be obtained by converting the ECEF coordinate system to the spherical coordinate.

$$\delta = \arcsin\left(\frac{z_{ECEF}}{\|r_{ECEF}\|}\right) \tag{8}$$

$$\alpha = \begin{cases} \arccos\left(\frac{1}{\cos \delta} \frac{x_{ECEF}}{\|r_{ECEF}\|}\right) & y_{ECEF} > 0 \\ -\arccos\left(\frac{1}{\cos \delta} \frac{x_{ECEF}}{\|r_{ECEF}\|}\right) & y_{ECEF} \leq 0 \end{cases} \tag{9}$$

2.4. Sub-Satellite Points Density along Latitude

To design a mega-constellation in which sub-satellite points are evenly distributed along the latitude zone, an indicator that measures the distribution density of sub-satellite points must first be established. Therefore, we define the density of a constellation’s sub-satellite points along latitude as the number of sub-satellite points per unit latitude zonal area of the Earth’s surface. Its expression is as follows:

$$D = \frac{n}{S} \tag{10}$$

where S represents the area of an arbitrary latitude zone on the Earth’s surface, as shown in the shadow section in Figure 1. n is the number of sub-satellite points falling within the S region.

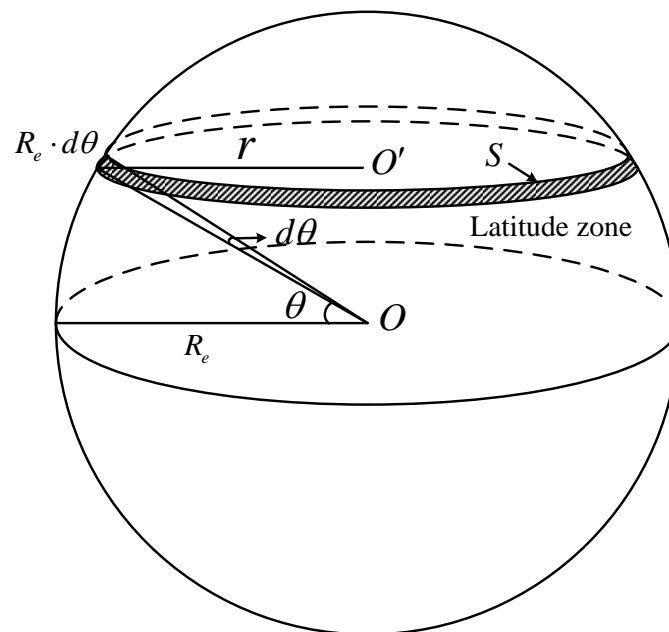


Figure 1. Schematic diagram of a latitude zone on the Earth’s surface.

Before calculating the area of the S , the necessary assumptions must be given. Consider the Earth as an ideal sphere. The radius of the Earth is taken to be 6378.137 km (Earth’s equatorial radius). The area of latitude range $[\delta, \delta + \Delta\delta]$. can be computed with area integral and expressed by the following equation.

$$S = \int_{\delta}^{\delta+\Delta\delta} 2\pi r R_e \cdot d\theta = \int_{\delta}^{\delta+\Delta\delta} 2\pi r R_e^2 \cos \theta \cdot d\theta = 2\pi R_e^2 \cdot [\sin(\delta + \Delta\delta) - \sin \delta]. \tag{11}$$

Suppose the Earth’s surface is divided into m latitude zones. The density of the constellation’s sub-satellite points on the k -th latitude zone at time t is denoted as $D_{k,t}$.

Taking Δt as the time step, then in an orbital period T , the average density of the sub-satellite point at each time in the k -th latitude zone is:

$$\bar{D}_k = \frac{\Delta t}{T} \sum_{i=0}^{n_{\Delta t}} D_{k,i \cdot \Delta t} \quad (12)$$

where $n_{\Delta t} = T/\Delta t$, indicates the sampling size in the orbital period T .

The probability density function of \bar{D}_k can be expressed as:

$$f_k = \frac{\bar{D}_k}{\sum_{i=1}^m \bar{D}_i} \quad (13)$$

Walker constellation features high symmetry and uniform satellite phases distribution on the same orbit plane, ensuring its configuration remains stable during operation. According to these characteristics, it can be reasonably deduced that for the Walker constellations, the value of f_k is influenced by (a, e, i) and is independent of (N, P, F) .

2.5. Mega-Constellation Configuration Design

To achieve uniform global coverage, this paper constructs a mega-constellation composed of multiple sub-Walker constellations with the same semimajor axis, eccentricity, argument of perigee, and different orbital inclination. For the Walker constellation, the satellite's inclination limits the latitude range of the sub-satellite points distribution, and the latitude boundary is $[-i, i]$. Moreover, its sub-satellite points are densely distributed in high latitudes while sparsely in low. Based on these characteristics, the following mega-constellation design strategy is proposed. Firstly, utilize a large inclination Walker constellation to cover the high latitude region. Then, based on the density of sub-satellite points in high latitudes, the parameters of sub-constellation with small inclination are deduced in turn. A mixed Walker constellation with the same sub-satellite points density at each latitude zone will eventually be obtained. In addition, all satellites are designed to be in prograde orbit to ensure orderly operation within the mega-constellation.

Figure 2 depicts the process of developing a mega-constellation using the method proposed in this paper. The specific implementation steps are shown as follows:

Step1: Set initial parameters for mega-constellations design. Dividing the Earth's surface into m latitude zones, the latitude span of each latitude zone is: $\Delta\delta = \frac{\pi}{m}$. The area of latitude zone from north to south is: S_1, S_2, \dots, S_m . Then, with $\Delta\delta$ as the unit, the sub-constellation is constructed in turn. The inclination of sub-constellation in descending order is: $\frac{\pi}{2}, \frac{\pi}{2} - \Delta\delta, \frac{\pi}{2} - 2\Delta\delta, \dots, \frac{\pi}{2} - (\frac{m}{2} - 1)\Delta\delta$. In this order, the sub-constellations are denoted as $C_1, C_2, \dots, C_{m/2}$. (Mega-constellation C consists of $\frac{m}{2}$ sub-constellations since the Walker constellation is symmetrical in the southern and northern hemispheres. In other words, the constellation design only needs to meet the uniform distribution of sub-satellite points density in the northern hemisphere to achieve global uniform distribution.)

Step2: Set the total number of satellites N_{C_1} in the Walker constellation with maximum orbital inclination ($i = 90^\circ$). Calculate the average density \bar{D}_{k,C_1} of the sub-constellations C_1 in each latitude zone. $j = 2$.

Step3: Based on the initial sub-constellations and Equation (14), the average number of sub-satellite points in the northernmost latitude zone of the j -th sub-constellation can be determined by Equation (15).

$$\bar{D}_{1,C} = \bar{D}_{j,C} + \bar{D}_{1,C_j} \quad (14)$$

$$n_{1,C_j} = \frac{\bar{n}_{1,C_1} \cdot S_j}{S_1} - \bar{n}_{j,C} \quad (15)$$

where $\bar{n}_{j,C}$ is the average number of sub-satellite points of mixed constellation C falling on the j -th latitude zone.

Step4: According to n_{1,C_j} , the average distribution number of the C_j in the k -th latitude zone $k = 2, 3, \dots, m - j + 1$ can be obtained:

$$n_{k,C_j} = \frac{n_{1,C_j} \cdot S_{k+j-1} \cdot f_{k,C_j}}{S_j \cdot f_{1,C_j}} \tag{16}$$

where f_{k,C_j} represents the probability density of C_j for the density of sub-satellite points in the k -th latitude zone.

Total satellites number of C_j can be calculated by adding the number of sub-satellite points on each latitude zone.

$$N_{C_j} = \sum_{k=1}^m n_{k,C_j} \tag{17}$$

Step5: The mixed constellation C composed of j sub-constellations is obtained. Calculate the average number of sub-satellite points in each latitude zone of C and update $\bar{n}_{1,C}, \bar{n}_{2,C}, \dots, \bar{n}_{m,C}$.

$$\bar{n}_{m,C} = \sum_{k=1}^m n_{k,C_{m-k+1}} \tag{18}$$

Step6: If $j < m/2$, repeat Step3~Step5, $j = j + 1$. Otherwise, continue in step 7.

Step7: Output the number of satellites contained in each sub-constellation, $N_{C_1}, N_{C_2}, \dots, N_{C_{\frac{m}{2}}}$, respectively.

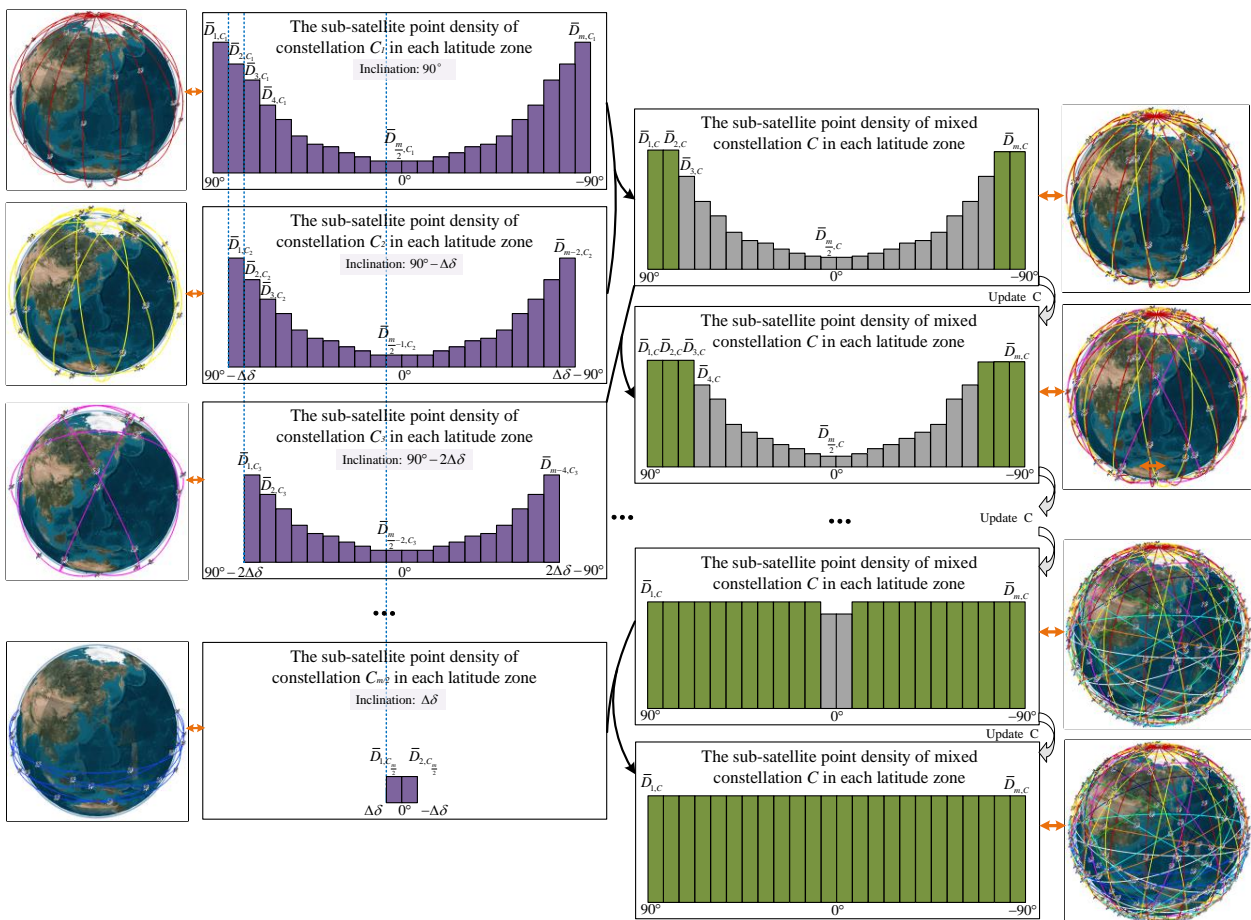


Figure 2. Schematic diagram of sub-constellation generation according to the sub-satellite point density of constellation in iterative order.

The configuration of a Walker constellation depends on the three parameters (N , P , and F). Through the above steps, we obtain the N of all sub-constellations in the mixed Walker constellation and ensure that the sub-satellite points of the mega-constellation are evenly distributed along latitude. The next work is to determine the P of each sub-constellation and guarantee that the sub-satellite points of the mega-constellation are relatively uniformly distributed along the longitude direction. When the number of satellites is huge, the F has little impact on the constellation configuration. Therefore, the F can be selected within a reasonable range.

For the Walker constellation with a given N , the smaller the deviation between the right ascension of ascending node (RAAN) difference of the adjacent orbits and the phase difference between the adjacent satellites in the same orbit plane, the more evenly the constellation's sub-satellite points spread globally. Meanwhile, considering collision avoidance between satellites, the constraint must be satisfied that the RAAN difference of any two satellites in the same Walker constellation cannot be equal to 180° . As a result, the orbital plane number of the j -th sub-constellation is determined by:

$$P_{C_j} = \left\{ P \mid \min \left(2\pi \left| \frac{1}{P} - \frac{P}{N_{C_j}} \right| \right), \text{mod}(N_{C_j}, P) = 0, \text{mod} \left(\pi, \frac{2\pi}{P} \right) \neq 0 \right\}$$

The parameter Ω_0 defines the constellation's positional datum. Once the Ω_0 has been determined, the absolute position between sub-constellations can be established. To make each sub-constellation uniformly distributed, set the Ω_0 of the j -th sub-constellation to $4\pi j/m$.

2.6. Constraints on Collision Avoidance

This paper deduces the minimum distance between the two satellites in the near-circular orbit with the same altitude to avoid collisions between satellites within the mega-constellation. Supposing that the minimum distance is greater than the safe distance between satellites, in that case, it is regarded that the two satellites will not collide.

Figure 3 shows the spatial geometric relationship between satellites S_1 and S_2 in the ECI coordinate system. $i_1, i_2, u_1, u_2, \Omega_1, \Omega_2$ express the inclination, the argument of latitude, and RAAN of satellite S_1 and S_2 , respectively. Furthermore, $u_1 = \angle MOS_1, u_2 = \angle POS_2, \delta_1 = \angle NOS_1, \delta_2 = \angle QOS_2, \alpha_1 = \angle MTN, \alpha_2 = \angle PTQ$. ρ is the geocentric angle between two satellites, and $\rho = \angle S_1OS_2$.

According to the sine theorem of the spherical triangle, in ΔMNS_1 and ΔPQS_2 , the following relationship can be derived.

$$\begin{cases} \sin \delta_1 = \sin u_1 \cdot \sin i_1 \\ \sin \delta_2 = \sin u_2 \cdot \sin i_2 \end{cases} \tag{19}$$

In ΔMTS_1 and ΔPTS_2 , by the sine and cosine theorems, Equations (20) and (21) can be obtained:

$$\begin{cases} \sin \alpha_1 = \sin u_1 \cdot \frac{\cos i_1}{\cos \delta_1} \\ \sin \alpha_2 = \sin u_2 \cdot \frac{\cos i_2}{\cos \delta_2} \end{cases} \tag{20}$$

$$\begin{cases} \cos u_1 = \sin \left(\frac{\pi}{2} - \delta_1 \right) \cdot \cos \alpha_1 = \cos \delta_1 \cdot \cos \alpha_1 \\ \cos u_2 = \sin \left(\frac{\pi}{2} - \delta_2 \right) \cdot \cos \alpha_2 = \cos \delta_2 \cdot \cos \alpha_2 \end{cases} \tag{21}$$

Set $\angle S_1TS_2 = A$, easily found Equation (22) from the geometric relationship.

$$A = \Omega_2 + \alpha_2 - (\Omega_1 + \alpha_1) = \Delta\Omega + \Delta\alpha \tag{22}$$

The expression for the geocentric angle is:

$$\begin{aligned} \cos \rho &= \cos \left(\frac{\pi}{2} - \delta_1 \right) \cdot \cos \left(\frac{\pi}{2} - \delta_2 \right) + \sin \left(\frac{\pi}{2} - \delta_1 \right) \cdot \sin \left(\frac{\pi}{2} - \delta_2 \right) \cdot \cos A \\ &= \sin \delta_1 \cdot \sin \delta_2 + \cos \delta_1 \cdot \cos \delta_2 \cdot \cos A \end{aligned} \tag{23}$$

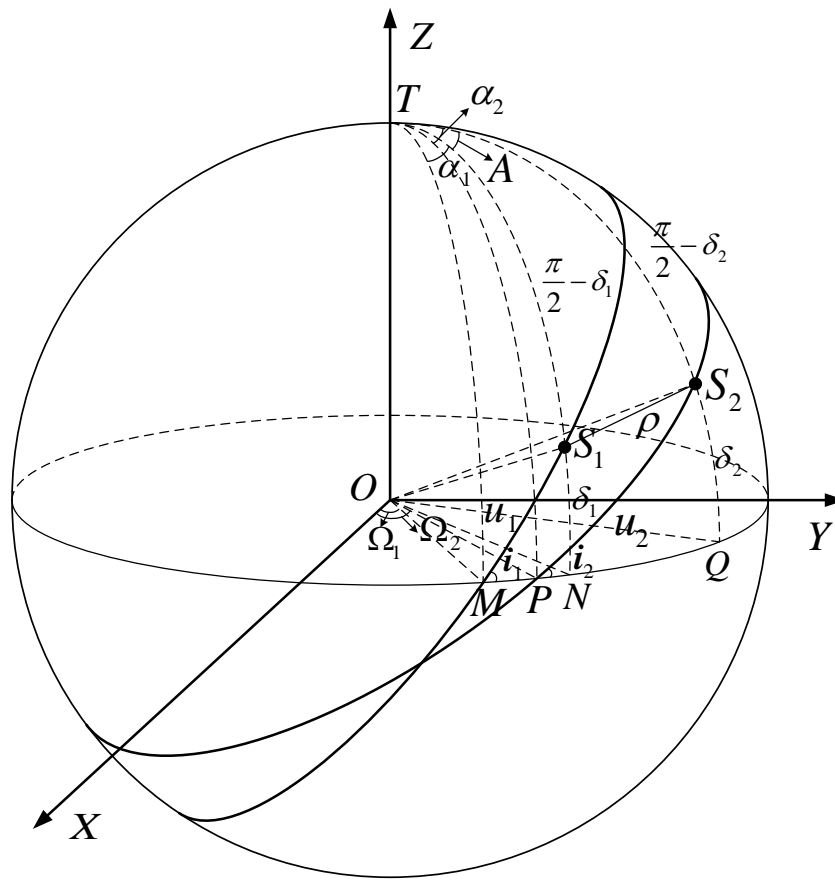


Figure 3. Schematic diagram of the spatial geometry of any two satellites in the ECI coordinate system.

Combining Equations (20)–(22), the expression of $\cos A$ can be derived.

$$\begin{aligned} \cos A &= \frac{\cos \Delta\Omega}{\cos \delta_1 \cdot \cos \delta_2} (\cos u_1 \cdot \cos u_2 + \cos i_1 \cdot \cos i_2 \cdot \sin u_1 \cdot \sin u_2) \\ &\quad - \frac{\sin \Delta\Omega}{\cos \delta_1 \cdot \cos \delta_2} (\cos u_1 \cdot \sin u_2 \cdot \cos i_2 + \sin u_1 \cdot \cos u_2 \cdot \cos i_1) \end{aligned} \quad (24)$$

Ultimately, the expression for $\cos \rho$ is arrived by combining Equations (19) and (24)

$$\begin{aligned} \cos \rho &= \sin u_1 \cdot \sin u_2 \cdot \sin i_1 \cdot \sin i_2 + \cos \Delta\Omega \cdot (\cos u_1 \cdot \cos u_2 + \cos i_1 \cdot \cos i_2 \cdot \sin u_1 \cdot \sin u_2) \\ &\quad - \sin \Delta\Omega \cdot (\cos u_1 \cdot \sin u_2 \cdot \cos i_2 - \sin u_1 \cdot \cos u_2 \cdot \cos i_1) \end{aligned} \quad (25)$$

Since the phase difference between the two satellites is fixed, $u_1 + \Delta u$ can be used to replace u_2 . Substitute k_1, k_2, k_3, k_4 for the known constants in Equation (25) to simplify the expression.

$$\begin{aligned} \cos \rho &= k_1 \sin u_1 \cdot \sin(u_1 + \Delta u) + k_2 \cos u_1 \cdot \cos(u_1 + \Delta u) \\ &\quad + k_3 \cos u_1 \cdot \sin(u_1 + \Delta u) + k_4 \sin u_1 \cdot \cos(u_1 + \Delta u) \end{aligned}$$

$$\begin{cases} k_1 = \sin i_1 \cdot \sin i_2 + \cos \Delta\Omega \cdot \cos i_1 \cdot \cos i_2 \\ k_2 = \cos \Delta\Omega \\ k_3 = -\sin \Delta\Omega \cdot \cos i_2 \\ k_4 = \sin \Delta\Omega \cdot \cos i_1 \end{cases} \quad (26)$$

The formula is further simplified by expanding Δu and replacing the constants in Equation (26) with a, b, c .

$$\begin{aligned} \cos \rho &= (k_1 \sin u_1 - k_4 \sin \Delta u) \sin^2 u_1 + (k_2 \cos \Delta u + k_3 \sin \Delta u) \cos^2 u_1 \\ &\quad + (k_1 \sin \Delta u - k_2 \sin \Delta u + k_3 \cos \Delta u + k_4 \cos \Delta u) \sin u_1 \cdot \cos u_1 \end{aligned} \quad (27)$$

where

$$\begin{cases} a = k_1 \cos \Delta u - k_4 \sin \Delta u \\ b = k_2 \cos \Delta u + k_3 \sin \Delta u \\ c = k_1 \sin \Delta u - k_2 \sin \Delta u + k_3 \cos \Delta u + k_4 \cos \Delta u \end{cases}$$

The final equation for $\cos \rho$ concerning u_1 is as follows:

$$\cos \rho = a \sin^2 u_1 + b \cos^2 u_1 + c \sin u_1 \cdot \cos u_1 \tag{28}$$

The $\cos \rho$ in Equation (28) can be transformed as:

$$\cos \rho = \frac{a + b}{2} + \frac{b - a}{2} \cos(2u_1) + \frac{c}{2} \sin(2u_1) \tag{29}$$

For the expression $f(x, y) = x \cos \theta + y \sin \theta$ with $\theta \in [0, 2\pi]$, the $f(x, y)$ can take the maximum value when the unit vector $(\cos \theta, \sin \theta)$ and the vector (x, y) are parallel and in the same direction. At this point, the vector $(\cos \theta, \sin \theta)$ can be expressed as:

$$(\cos \theta, \sin \theta) = \left(\frac{x}{\sqrt{x^2 + y^2}}, \frac{y}{\sqrt{x^2 + y^2}} \right)$$

At this particular point, the $f(x, y)$ is expressed as:

$$x \cdot \frac{x}{\sqrt{x^2 + y^2}} + y \cdot \frac{y}{\sqrt{x^2 + y^2}} = \sqrt{x^2 + y^2}$$

Applying this result to our maximization problem yields, the maximum value of $\cos \rho$ is:

$$\max(\cos \rho) = \frac{a + b}{2} + \frac{\sqrt{(b - a)^2 + c^2}}{2} \tag{30}$$

Similarly, the minimum value of $\cos \rho$ can be obtained as follows:

$$\min(\cos \rho) = \frac{a + b}{2} - \frac{\sqrt{(b - a)^2 + c^2}}{2} \tag{31}$$

When $\cos \rho$ takes the minimum (maximum) value, the geocentric angle between the two satellites reaches the maximum (minimum), and the distance between the two satellites is also the maximum (minimum).

The minimum distance between the two satellites is:

$$d_{min} = 2(R_e + H) * \sin \left(\frac{1}{2} \arccos \left(\frac{a + b}{2} + \frac{\sqrt{(b - a)^2 + c^2}}{2} \right) \right) \tag{32}$$

It is easy to obtain the maximum distance between any two satellites.

$$d_{max} = 2(R_e + H) * \sin \left(\frac{1}{2} \arccos \left(\frac{a + b}{2} - \frac{\sqrt{(b - a)^2 + c^2}}{2} \right) \right) \tag{33}$$

If the minimum distance between two satellites is less than the safe distance. Then, adjust the argument of latitude of either satellite until the minimum distance between it and all other satellites is greater than the safe distance.

3. ISLs Design

Due to the rapid change in relative positions between LEO satellites, the ISLs between satellites in different orbital planes are of short duration, which tends to cause frequent

link switching. This not only poses a major technical challenge to the recapture, targeting, and tracking of satellites, but also hinders the smooth operation of inter-satellite communication networks. In this case, this paper establishes ISLs based on the principle of full period visibility of the satellites and minimization of the maximum inter-satellite distance. This approach assures the permanence of the link between the satellites and avoids link reconstruction during data transmission.

In this section, based on the design of the mega-constellation in this paper, we propose a solution for establishing stable ISLs between the satellites to ensure that any two satellites can communicate efficiently

3.1. Visibility Conditions between Satellites

Figure 4 shows the spatial geometric relationship of the two satellites. Vector r_1 , r_2 , denotes the positions of satellites A and B, respectively. h is the distance from the line of sight of two satellites to the Earth's center. Then, the visibility conditions of the two satellites can be expressed as follows: If h is greater than the radius of the Earth, the two satellites are visible to each other. h is calculated as:

$$h = \frac{|r_1| \cdot |r_2| \cdot \sin \theta}{|r_1 - r_2|}$$

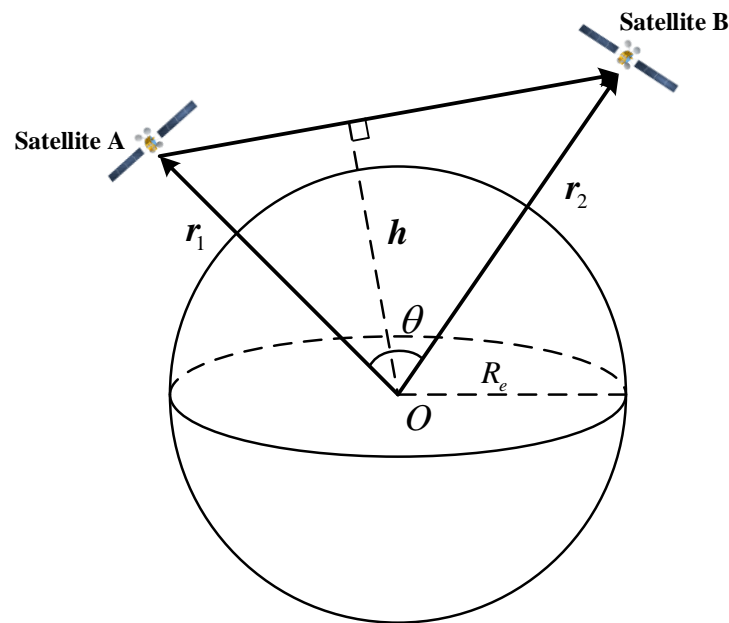


Figure 4. The visibility geometry of any two satellites in space.

3.2. Global Connectivity

Mega-constellations need to meet global connectivity requirements to communicate between any two locations via satellite nodes. Applying adjacency matrix in graph theory to describe and analyze the connectivity of satellite nodes is a valuable method [42]. The adjacency matrix [43] of ISLs can be expressed as:

$$A = \begin{bmatrix} a_{11} & a_{12} & \dots & a_{1N_s} \\ a_{21} & a_{22} & \dots & a_{2N_s} \\ \vdots & \vdots & \vdots & \vdots \\ a_{N_s1} & a_{N_s2} & \dots & a_{N_sN_s} \end{bmatrix}$$

where N_s is the total number of satellites contained in the mega-constellation, and a_{ij} indicates whether there is an ISL between the i -th satellite and the j -th satellite. If there is

an ISL between two satellites, then the element in the corresponding position of matrix A is set to 1. Otherwise, it is set to 0.

The judgment matrix can be constructed by utilizing the adjacency matrix, which can be employed to analyze the connectivity of ISLs. The judgment matrix is given by

$$R = A + A^2 + \dots + A^{N_s-1}.$$

A sufficient condition for global connectivity of a mega-constellation is that all elements of the matrix R are not zero. In addition, the element R_{ij} indicates the number of different paths from the i -th satellite to the j -th satellite.

3.3. Intersatellite Links Design

The highly dynamic nature of LEO satellites makes frequent switching of the earth-satellite and inter-satellite links inevitable. Link switching poses many negative effects on inter-satellite data transmission. For one, the large amount of pathfinding information generated by link switching is easy to cause network congestion. Secondly, the high latency of satellite rerouting and the high rate of data loss significantly reduce the utilization of the network. Therefore, it makes sense to prevent link switching. In this section, based on the mega-constellation configuration proposed in this paper, a solution is presented for designing the ISLs without inter-satellite link switching.

Assuming that l ISLs are established on each satellite, the procedures of ISLs design is as follows:

Step1: Referring to Section 2.6, calculate the maximum distance between any two satellites in the mega-constellation. Then, construct a matrix D_{max} of the maximum distances between satellites.

$$D_{max} = \begin{bmatrix} 0 & d_{max}^{1,2} & \dots & d_{max}^{1,N_s} \\ 0 & 0 & \dots & d_{max}^{2,N_s} \\ \vdots & \vdots & \ddots & \vdots \\ 0 & 0 & \dots & d_{max}^{N_s-1,N_s} \\ 0 & 0 & \dots & 0 \end{bmatrix}$$

where $d_{max}^{i,j}$ is the maximum distance between the i -th satellite and the j -th satellite.

Step2: The elements in the matrix D_{max} that do not meet the visible condition are denoted as 0, and they form a new matrix D'_{max} .

Step3: Establish an adjacency matrix A , which contains the ISLs information between satellites. The initial state of A is a zero matrix of order $N_s \times N_s$, $i = 1$.

Step4: Starting with the i -th row of D'_{max} , sort the row data in descending order. Record the location information of the first l smallest element in D'_{max} . Then, the elements in the corresponding position of A are assigned to 1, and the symmetric position of these elements in A is also set to 1.

Step5: Calculate the sum of rows and columns of matrix A . The sum of the elements in the j -th row or the k -th column is denoted as Row_j and Col_k , respectively. If $Row_j = l$ or $Col_k = l$, the j -th satellite or the k -th satellite will no longer participate in subsequent calculations.

Step6: if $i < N_s$, then, $i = i + 1$, and repeat Step4 and Step5. Otherwise, terminate the loop.

Step7: Output the adjacency matrix A that contains ISLs information.

The above ISLs design steps produce a network where each satellite has a fixed ISL to the other l satellites. Each ISL in the mega-constellation is capable of ensuring full-time-domain interconnection. This stable link formation allows data to be transmitted over the satellite without switching links.

3.4. Shortest Path Transmission

Determining the data transmission path between two satellites is essential for the LEO mega-constellations system. According to graph theory, the topology of a mega-constellation can be abstracted as a time-varying undirected graph, represented as:

$$\begin{cases} G = (V, E) \\ V = \{v_i | v_i \in (v_1, v_2, \dots, v_{N_s})\} \\ E = \{(v_i, v_j) | v_i, v_j \in V\} \end{cases}$$

where V denotes the set of satellite nodes, and E is the set of edges between satellite nodes.

The widely used shortest path first protocol (SPF) is the basis of end-to-end low-latency transmission. Dijkstra algorithm [44] is a well-known and effective method for finding the shortest path in the network. Figure 5 shows the pseudo-code of the algorithm.

```

Input: Directed graph  $G$  and Source node  $S$ 
Output: All the shortest paths from the source vertex to every vertex in  $V$ 
1: for each vertex  $v$  in  $G$ :
2:    $dist[v] = \text{infinity}$                                 % initial distance from source to vertex  $v$  is set to infinite
3:    $previous[v] = \text{undefined}$                           % Previous node in optimal path from source
4:    $dist[S] = 0$                                         % Distance from source to source
5:    $Q = \text{the set of all nodes in } G$                   % all nodes in the graph are unoptimized - thus are in  $Q$ 
6:   While  $Q$  is not empty:
7:      $u = \text{node in } Q \text{ with smallest } dist[ ]$ 
8:     remove  $u$  from  $Q$ 
9:     for each neighbor  $v$  of  $u$ :
10:       $alt = dist[u] + dist\_between(u,v)$ 
11:      if  $alt < dist[v]$ 
12:         $dist[v] = alt$ 
13:         $previous[v] = u$ 
14:   return  $previous[ ]$ 

```

Figure 5. Pseudo-code for Dijkstra's algorithm.

4. Simulation and Results

To verify the effectiveness of the mega-constellation design method proposed in this paper, we carry out simulation experiments and contrastive analysis.

In the simulation, a circular orbit is used for constellation design to maintain inter-satellite and satellite-ground communication's constant signal strength. Therefore, the orbit elements e and the ω are set to 0.

4.1. Simulation Studies and Results on Mega-Constellation Design

The probability density function of the sub-satellite points density f_k is the key variable in the mega-constellation design method proposed in this paper. During the constellation design process, we regard it as a variable that only relates to the satellite's orbital elements, not interested in constellation parameters. By default, Walker constellations with the same other parameters but different numbers of satellites have the same f_k . To verify that the statement is reasonable, this paper conducts a simulation analysis on the distribution characteristics of f_k .

Figure 6 shows the simulation results about the f_k . The parameters are set as follows: $e = 0$, $H = 600 \text{ km}$, $\omega = 0$. The number of orbital planes is equal to the total number of satellites in the Walker constellation ($F = 1$). These parameters apply to all subgraphs in Figure 6. The four groups of figures respectively represent the distribution of sub-

satellite points density of Walker constellation under different orbit inclinations. The three subgraphs of each group compare the distribution of f_k when all other parameters are the same but for the total number of satellites, and show the deviation rate between the two. By comparing the four groups of figures, it can be seen that the f_k distributions corresponding to different orbit inclination vary considerably. In Figure 6a, the distribution of f_k is almost identical whether the total number of satellites in the Walker constellation is 300 or 500. The deviation rate between the two sets of data is kept within 2%. Therefore, it can be concluded that the total number of satellites makes almost no difference to f_k . The same conclusion can be drawn for the other three sets of figures. To sum up, it is reasonable to assume that the distribution of f_k is independent of the total number of satellites in the Walker constellation as a precondition for the mega-constellation design in this paper.

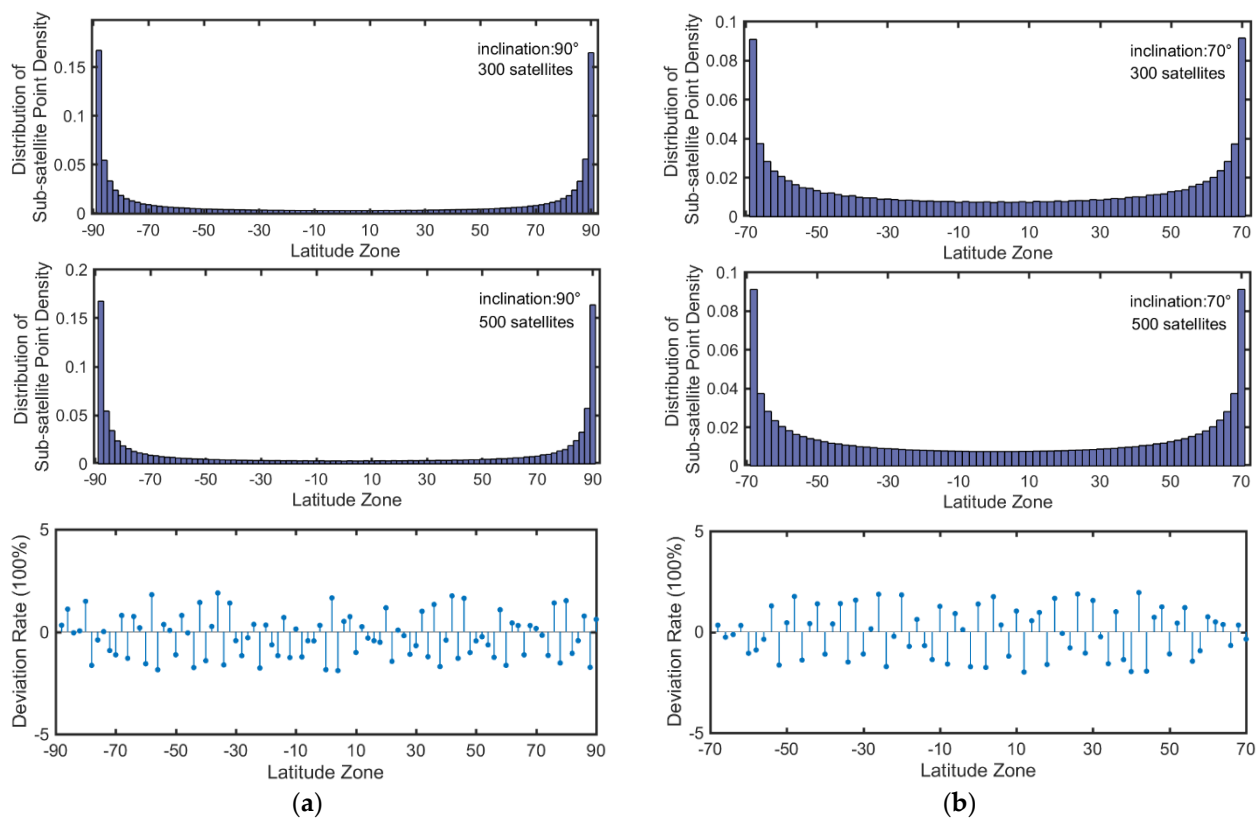


Figure 6. Cont.

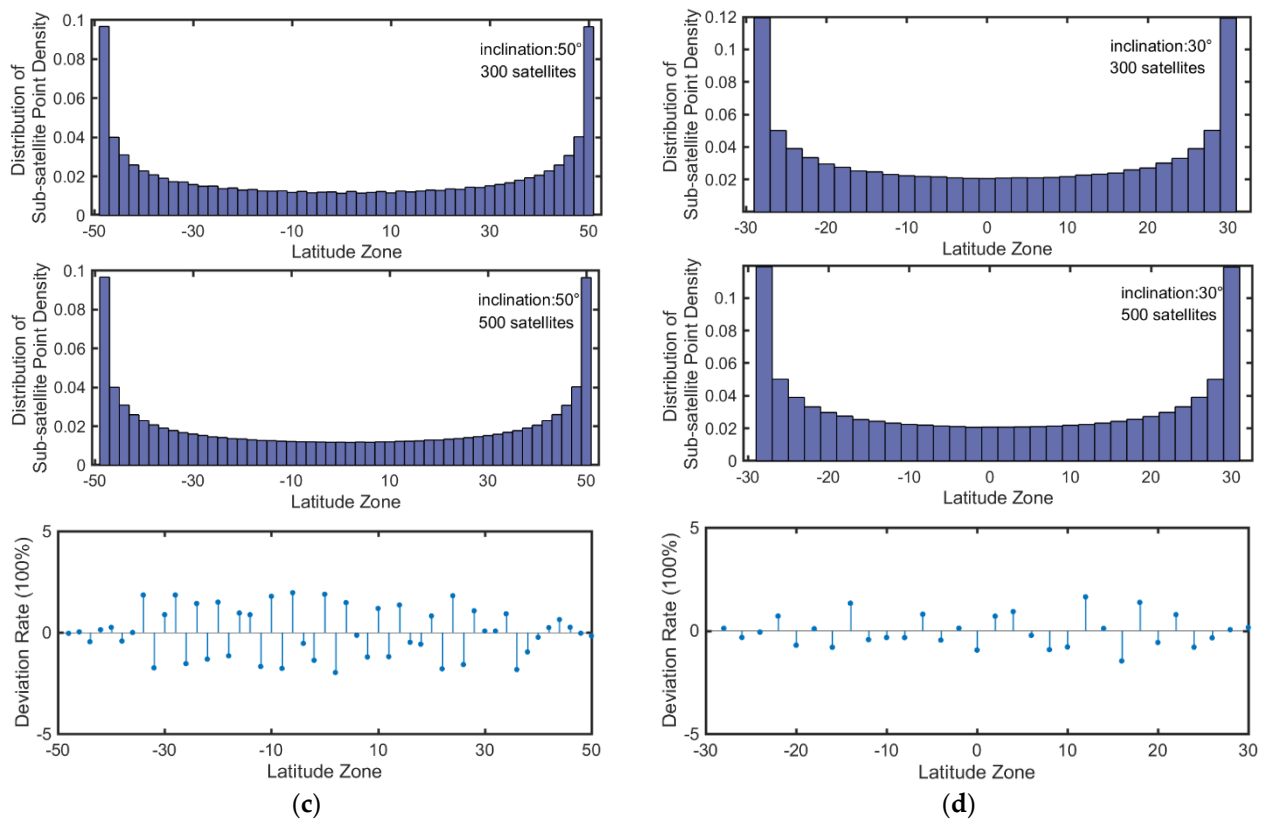


Figure 6. Distribution of sub-satellite points density along latitude zones with the variation of the total number of satellites and the orbital inclination. (a) Constellation with an orbital inclination of 90°; (b) Constellation with an orbital inclination of 70°; (c) Constellation with an orbital inclination of 50°; (d) Constellation with an orbital inclination of 30°.

Simulations are carried out according to the mega-constellation design method proposed in this paper. The orbit altitude of all satellites is set to 600 km. The simulation duration is one orbital period, i.e., 96.69 min, and the time step is 1 min. A latitude zone is divided every 2°. The total number of satellites in the initial sub-constellation with the maximum orbit inclination (90°) is set to 150. After iterative calculations, an LEO mega-constellation composed of 45 sub-Walker constellations with 5686 satellites is finally achieved. Table 1 records the results of the mega-constellation configuration obtained by the method proposed in this paper.

Table 1. Simulation results of the mega-constellation configuration.

Sub-Constellation Number	<i>i N P</i>	Sub-Constellation Number	<i>i N P</i>
Cons_1	90° 150 15	Cons_24	44° 138 23
Cons_2	88° 183 3	Cons_25	42° 131 131
Cons_3	86° 184 23	Cons_26	40° 126 9
Cons_4	84° 190 19	Cons_27	38° 123 3
Cons_5	82° 196 14	Cons_28	36° 118 59
Cons_6	80° 188 47	Cons_29	34° 112 14
Cons_7	78° 184 23	Cons_30	32° 104 13
Cons_8	76° 194 97	Cons_31	30° 98 7
Cons_9	74° 184 23	Cons_32	28° 95 5
Cons_10	72° 195 13	Cons_33	26° 90 9

Table 1. Cont.

Sub-Constellation Number	<i>i N P</i>	Sub-Constellation Number	<i>i N P</i>
Cons_11	70° 187 11	Cons_34	24° 80 5
Cons_12	68° 182 13	Cons_35	22° 75 5
Cons_13	66° 173 173	Cons_36	20° 69 3
Cons_14	64° 184 23	Cons_37	18° 58 29
Cons_15	62° 173 173	Cons_38	16° 58 29
Cons_16	60° 173 173	Cons_39	14° 45 5
Cons_17	58° 168 14	Cons_40	12° 46 23
Cons_18	56° 164 41	Cons_41	10° 33 3
Cons_19	54° 160 16	Cons_42	8° 28 7
Cons_20	52° 156 13	Cons_43	6° 22 11
Cons_21	50° 152 19	Cons_44	4° 14 7
Cons_22	48° 148 37	Cons_45	2° 7 7
Cons_23	46° 148 37		
Total		5686	

After accomplishing the preliminary design of a mega-constellation, calculate the minimum distance between any two satellites in the constellation according to the collision-avoidance constraints. Set the safe distance between satellites to be 10 km. A total of 176 groups of satellites have been counted as having a minimum distance less than this safe distance. Adjust the argument of latitude of anyone satellite in each group using 1° steps until the minimum distance between that satellite and all other satellites is greater than the safe distance. Finally, a mega-constellation that avoids the risk of self-collision is available.

To illustrate the superiority of the mixed Walker constellation design approach proposed in this paper, we will compare it with the Walker constellation of the same magnitude. To this end, a Walker constellation was constructed with an orbital inclination of 90° , an orbital altitude of 600 km, and consisting of 75 orbital planes, each containing 75 satellites, for a total of 5625 satellites. Figure 7 shows the 3D configuration of the two constellations and the position of the sub-satellite points on the Mercator projection map. Firstly, a comparison of 3D space images shows that the Walker constellation is more regularly distributed in space. However, the dense distribution of satellites at high latitudes not only wastes space resources but also significantly increases the collisions risk between satellites within the constellation. The mixed Walker constellation designed by applying the method in this paper can spread relatively evenly over the surface of the celestial sphere. The satellites are roughly equally distributed over all latitude zones, greatly relieving the pressure of dense satellite distribution over high latitude regions. Secondly, comparing the 2D maps, it can be seen that the sub-satellite points of the Walker constellation are completely uniformly distributed on the map, but since the Mercator projection is equiangular, its deformation increases with increasing latitude when representing distances, which means that the phenomenon Walker's sub-satellite points are evenly distributed at high latitudes is seriously distorted. In contrast, the distribution of sub-satellite points of the mixed Walker constellation shows a gradual sparseness from low to high latitudes, which is more in line with the expectation that the constellation is uniform in space. Therefore, in terms of distribution, the mixed Walker constellation designed in this paper is more conducive to uniform global coverage of the Earth.

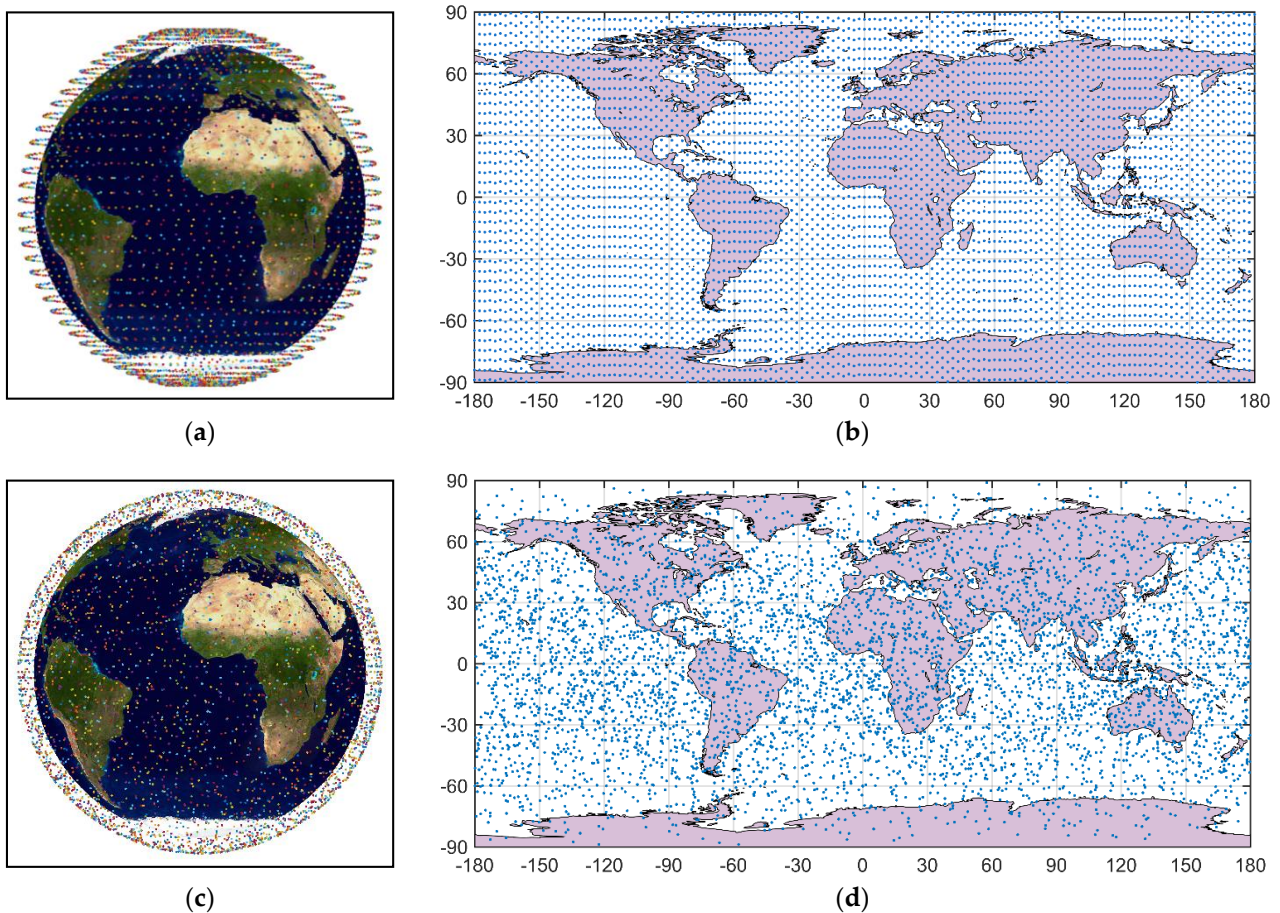


Figure 7. 2D and 3D comparison diagrams of the mixed Walker constellation and Walker constellation at the same amount. (a) 3D schematic of the Walker constellation with 5625 satellites; (b) 2D schematic of the Walker constellation with 5625 satellites; (c) 3D schematic of the mixed Walker constellation with 5686 satellites; (d) 2D schematic of the mixed Walker constellation with 5686 satellites.

To further demonstrate that the mixed Walker constellation effectively compensates for the uneven distribution of the Walker constellation along latitude, the sub-satellite point density of the two constellations along the latitude zone is calculated separately. The results are shown in Figure 8. In Figure 8a, the sub-satellite point density of the Walker constellation, which contains 5625 satellites, varies significantly across the latitude zones, with high latitudes being several times greater than low and middle latitudes. In contrast, the mixed Walker constellation of 5686 satellites has less difference in the density values of the sub-satellite points in each latitude zone, indicating a homogeneous distribution of satellites along latitude. It can be concluded that the mega-constellation designed in this paper effectively solves the problem of the uneven distribution of the Walker constellation on the latitudinal zone.

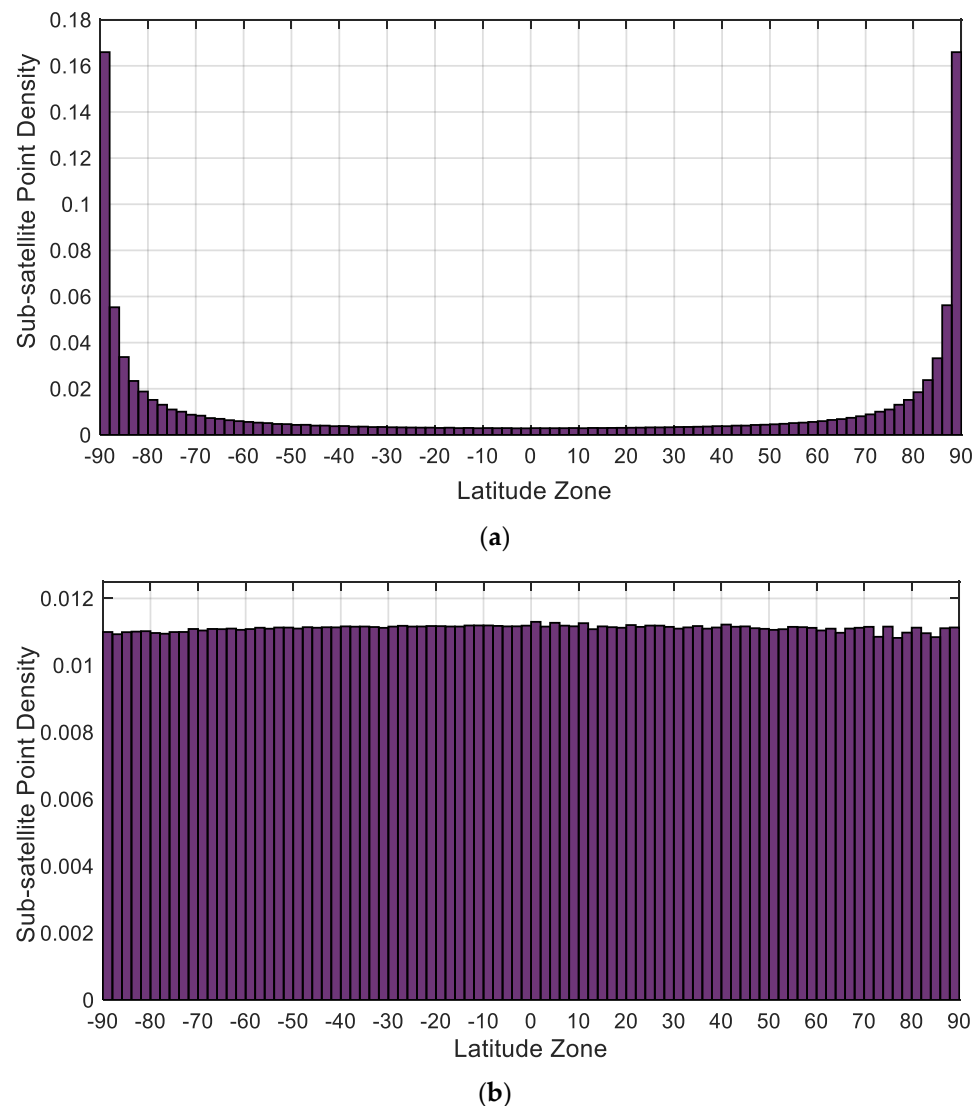


Figure 8. Comparison of the distribution of sub-satellite points density along latitude zones in the mixed Walker constellation and Walker constellation. (a) Distribution of sub-satellite points density along latitude zones of a Walker constellation with 5625 satellites; (b) Distribution of sub-satellite points density along latitude zones of a mixed Walker constellation with 5686 satellites.

The coverage performance is one of the most important indicators for evaluating the merits of a constellation design. The focus of the mega-constellation is on global coverage characteristics, for which the paper compares the N Asset Coverage of the Walker constellation with that of the mixed Walker constellation on a global scope. The resolution of the ground sampling points is $1^\circ \times 1^\circ$, and the field of view of the satellite for ground coverage is set to 50° . The simulation results are shown in Figure 9. In Figure 9a, the range of N Asset Coverage of the Walker constellation is 10~219, with a wide span of ground N Asset Coverage and more than 200 overlaps for the polar regions. However, in Figure 9b, the range of N Asset Coverage for the mixed Walker constellation is 18~25, with little variation in the number of duplicates covered across global regions. Figure 9c quantifies and compares the distribution of the N Asset Coverage between the two constellations, visually demonstrating the more concentrated distribution of the number of N Asset Coverage for the mixed Walker constellation. Furthermore, the N Asset Coverage distribution of the mixed Walker constellation peaks at 21 compared to 11 for the Walker constellation, indicating that for the same number of satellites, the mixed Walker constellation has a higher N Asset Coverage in most regions of the world. In conclusion, the mixed Walker

constellation designed in this paper has less variability in coverage performance across the globe than the Walker constellation and offers significant global coverage strengths.

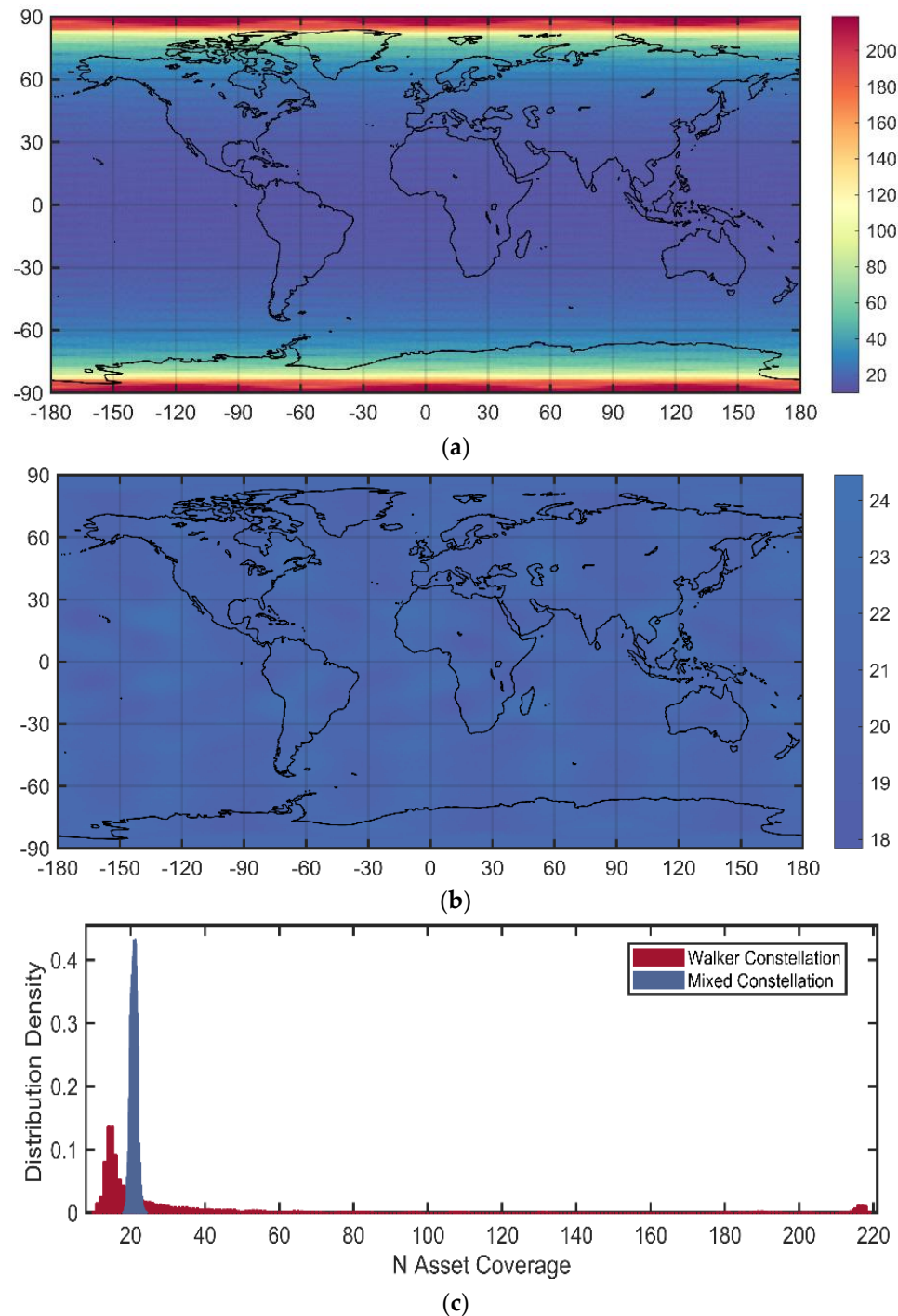


Figure 9. Global coverage performance of mixed Walker constellation vs. Walker constellation. (a) Distribution of N Asset Coverage around the globe for a Walker constellation with 5625 satellites; (b) Distribution of N Asset Coverage around the globe for a mixed Walker constellation with 5686 satellites; (c) Comparison of the distribution density of N Asset Coverage around the globe for the two mega-constellations.

4.2. Simulation Studies and Results on ISLs Scheme Design

In order to verify the effectiveness of the mega ISLs design method introduced in this paper, simulations are carried out to validate it. The results are shown in Figure 10. In

particular, Figure 10a–c represent a space diagram with three ISLs per satellite, for a total of 17,056 ISLs in the constellation. The subplots in the second and third rows of Figure 10 represent the loading of four and five ISLs per satellite for a total of 22,742 and 28,430 ISLs, respectively, in the constellation. To fully prove that the ISLs design can guarantee efficient data transmission between any two satellite nodes, three sets of satellites are arbitrarily selected for simulation analysis. The subgraphs in each column of Figure 10 enjoy the same set of source and target satellite nodes.

There is at least one ISL on each satellite in the constellation. It ensures that information can be passed between any two satellite nodes, which also means that the global connectivity requirements of the ISLs design are met. In addition, in terms of the information transmission path between the two satellites, this ISL design solution ensures that the two satellites can communicate with each other in a shorter path. Comparing the graphs vertically, it can be visualized that as the number of links established on each satellite increases, the pathfinding selectivity on each satellite node increases as well as the communication distance between the two satellites decreases. For example, in Figure 10b, when 3 links are built per satellite, the data transmission path between the two satellite nodes is very tortuous, but when the number of links is increased to 4 in Figure 10e, the communication path between the two satellite nodes is optimized to a greater extent.

Subplots in Figure 10j–l simulate the data transmission path distance variation for three sets of satellite nodes, respectively, with 600 s of continuous communication. Each subplot compares the case of three, four, and five links built on the satellite accordingly. The outcomes show that the ISLs design presented in this paper can provide continuous and stable communication between satellites. As the number of satellite links increases, the communication distance between the two satellites decreases, especially when the number of links increases from three to four, which can bring about a significant reduction in communication distance. However, when the number of onboard links increases from four to five, the reduction in communication distance is significantly reduced. Therefore, the number of links established on the satellite can be determined by weighing various factors such as technical complexity, construction costs, and quality of communication services. Based on the above analysis, the ISLs design based on the mixed Walker constellation proposed in this paper can achieve global connectivity as well as stable and efficient inter-satellite data transmission.

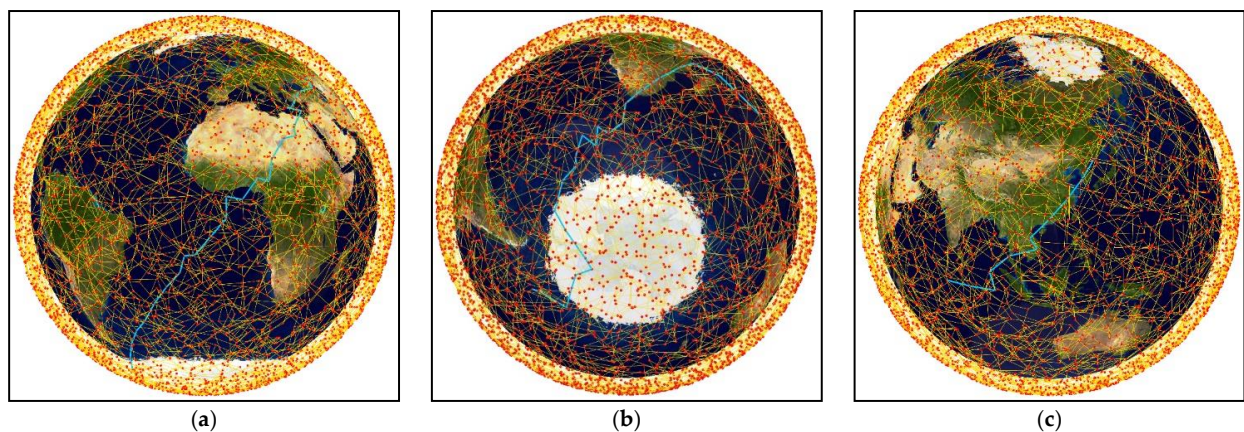


Figure 10. Cont.

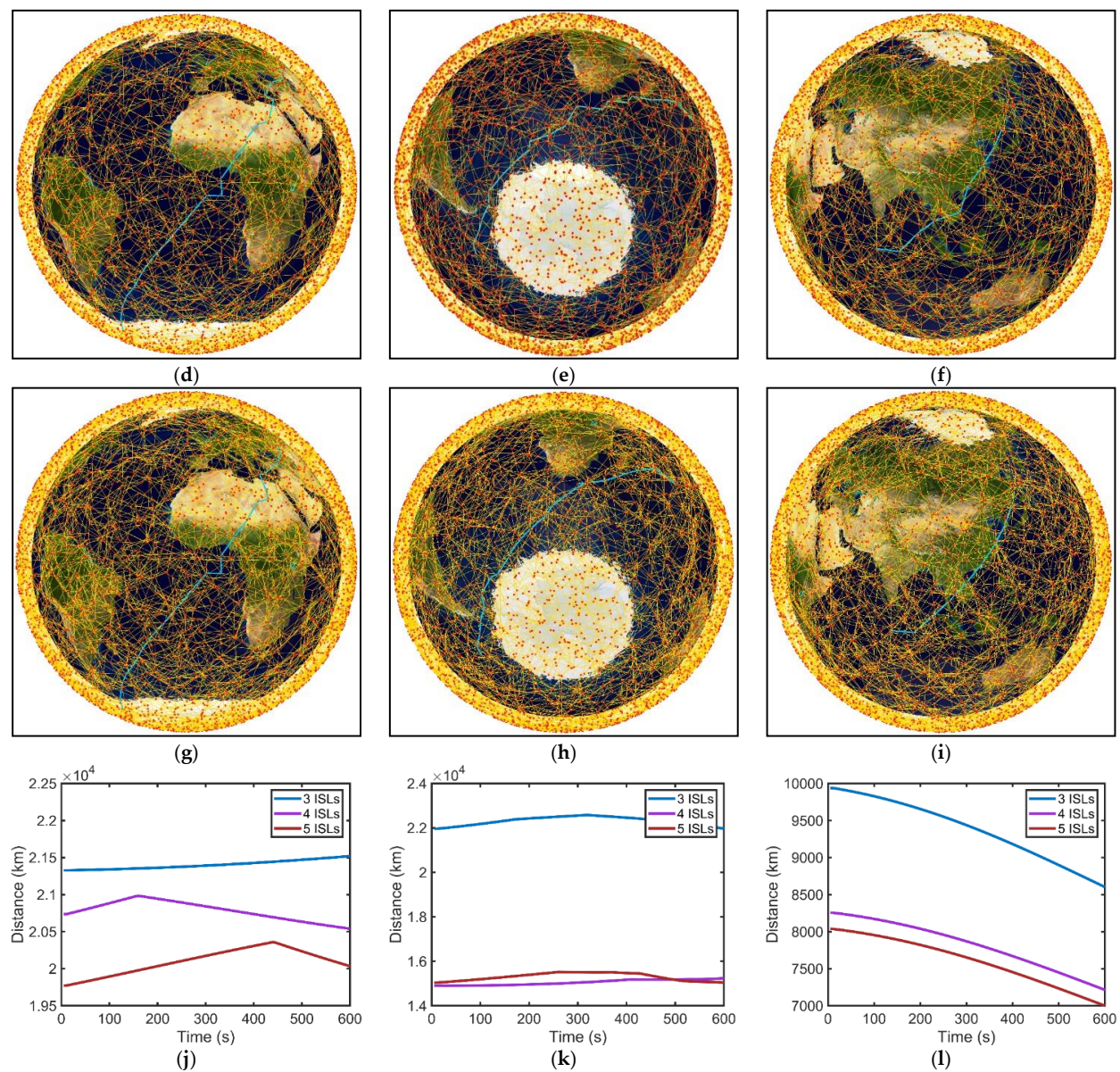


Figure 10. Comparison of data transmission paths on any 3 groups of satellite nodes in the mixed Walker constellation proposed in the paper with 3, 4, and 5 ISLs on the satellite, respectively. (a) 3 ISLs per satellite; (b) 3 ISLs per satellite; (c) 3 ISLs per satellite; (d) 4 ISLs per satellite; (e) 4 ISLs per satellite; (f) 4 ISLs per satellite; (g) 5 ISLs per satellite; (h) 5 ISLs per satellite; (i) 5 ISLs per satellite; (j) Comparison of 3 ISL schemes for continuous communication; (k) Comparison of 3 ISL schemes for continuous communication; (l) Comparison of 3 ISL schemes for continuous communication.

5. Conclusions

In view of the major shortcomings of conventional constellation configurations with uneven coverage on a global scale, this paper proposes a mixed Walker constellation design scheme for the same orbital layer that takes collision avoidance into account and effectively improves global coverage performance. On the basis of this constellation configuration, an ISLs design scheme is presented to guarantee efficient and stable inter-satellite data transmission. The main contributions of this paper are concluded as follows:

1. A model of a mega-constellation configuration with uniform global coverage has been developed, consisting of a mixture of Walker constellations with the same orbital altitude and different orbital inclinations. The simulation results show that the mixed

Walker constellation designed in this paper effectively compensates for the uneven distribution of the Walker constellation across the latitude zones and maintains a relatively balanced number of N Asset Coverage for all regions of the world. In addition, it has a higher number of N Asset Coverage than the Walker constellation of the same satellite magnitude in most parts of the world. It can be said that the mega-constellation designed in this paper has a superior global coverage performance.

2. During the design of the mega-constellations, we considered collision avoidance between satellites. This paper derives the minimum distance between any two satellites throughout their orbital period, based on space geometry and orbital dynamics theory. The collision-avoidance constraint is established at a safe distance. The orbital parameters of some satellites are adjusted so that the minimum distance between any two satellites in the mega-constellation is greater than the set safe distance.
3. Basis on the design of the mega-constellation configuration proposed in this paper, a scheme for the ISLs design is established according to the theory of the adjacency matrix in graph theory. This solution ensures that any two satellite nodes within the constellation can communicate in real-time. Moreover, the connection relationship of all satellite nodes is fixed. There is no need to switch links during data transmission, ensuring efficient and stable communication. Simulation results show that the communication distance between two satellite nodes decreases as the number of links on each satellite increases. Therefore, carrying as many ISLs on a satellite as conditions permit can improve the inter-satellite communication time efficiency.

Author Contributions: Conceptualization, L.J. and Y.Z.; data curation, L.J.; formal analysis, J.Y. and L.J.; funding acquisition, Y.Z.; investigation, L.J. and X.W.; methodology, L.J.; project administration, Y.Z.; supervision, Y.Z. and J.Y.; writing—original draft, L.J. All authors have read and agreed to the published version of the manuscript.

Funding: This research received no external funding.

Conflicts of Interest: The authors declare no conflict of interest.

References

1. Levchenko, I.; Xu, S.; Wu, Y.L.; Bazaka, K. Hopes and concerns for astronomy of satellite constellations. *Nat. Astron.* **2020**, *4*, 1012–1014. [[CrossRef](#)]
2. Ulybyshev, Y. Satellite constellation design for complex coverage. *J. Spacecr. Rockets* **2008**, *45*, 843–849. [[CrossRef](#)]
3. Reiland, N.; Rosengren, A.J.; Malhotra, R.; Bombardelli, C. Assessing and minimizing collisions in satellite mega-constellations. *Adv. Sp. Res.* **2021**, *67*, 3755–3774. [[CrossRef](#)]
4. Martin, W.L. Satellite-Constellation design. *J. Comput. Sci. Eng.* **1999**, *28*, 213–232.
5. Zhang, C.; Jin, J.; Kuang, L.; Yan, J. LEO constellation design methodology for observing multi-targets. *Astrodynamics* **2018**, *2*, 121–131. [[CrossRef](#)]
6. Walker, J.G. Continuous Whole-Earth by circular-orbit satellite patterns. *R. Aircr. Establ.* **1977**, *78*, 11169.
7. Ballard, A.H. Rosette Constellations of Earth Satellites. *IEEE Trans. Aerosp. Electron. Syst.* **1980**, *AES-16*, 656–673. [[CrossRef](#)]
8. Lang, T.J. Symmetric circular orbit satellite constellations for continuous global coverage. In Proceedings of the AAS/AIAA Astrodynamics Specialist Conference, Kalispell, MT, USA, 10–13 August 1987; pp. 1111–1132.
9. Lang, T.J.; Adams, W.S. *A Comparison of Satellite Constellations for Continuous Global Coverage*; Springer: Dordrecht, The Netherlands, 1998; pp. 51–62. [[CrossRef](#)]
10. Rider, L. Analytic Design of Satellite Constellations for Zonal Earth Coverage Using Inclined Circular Orbits. *J. Astronaut. Sci.* **1986**, *34*, 31–64.
11. Mortari, D.; Wilkins, M.P.; Bruccoleri, C. The flower constellations. *Adv. Astronaut. Sci.* **2003**, *115*, 269–290. [[CrossRef](#)]
12. Avendaño, M.E.; Davis, J.J.; Mortari, D. The 2-D lattice theory of Flower Constellations. *Celest. Mech. Dyn. Astron.* **2013**, *116*, 325–337. [[CrossRef](#)]
13. Davis, J.J.; Avendaño, M.E.; Mortari, D. The 3-D lattice theory of Flower Constellations. *Celest. Mech. Dyn. Astron.* **2013**, *116*, 339–356. [[CrossRef](#)]
14. Arnas, D.; Casanova, D.; Tresaco, E. 4D Lattice Flower Constellations. *Adv. Sp. Res.* **2021**, *67*, 3683–3695. [[CrossRef](#)]
15. Casanova, D.; Avendaño, M.; Mortari, D. Necklace theory on Flower Constellations. *Adv. Astronaut. Sci.* **2011**, *140*, 1791–1803.
16. Arnas, D.; Casanova, D.; Tresaco, E. 2D Necklace Flower Constellations. *Acta Astronaut.* **2018**, *142*, 18–28. [[CrossRef](#)]
17. Arnas, D.; Casanova, D.; Tresaco, E.; Mortari, D. 3-Dimensional Necklace Flower Constellations. *Celest. Mech. Dyn. Astron.* **2017**, *129*, 433–448. [[CrossRef](#)]

18. Arnas, D.; Casanova, D.; Tresaco, E. 2D Necklace Flower Constellations applied to Earth observation missions. *Acta Astronaut.* **2021**, *178*, 203–215. [[CrossRef](#)]
19. Huang, S.; Colombo, C.; Bernelli-Zazzera, F. Multi-criteria design of continuous global coverage Walker and Street-of-Coverage constellations through property assessment. *Acta Astronaut.* **2021**, *188*, 151–170. [[CrossRef](#)]
20. Zhang, T.J.; Shen, H.X.; Li, Z.; Qie, H.; Cao, J.; Li, H.N.; Yang, Y.K. Restricted constellation design for regional navigation augmentation. *Acta Astronaut.* **2018**, *150*, 231–239. [[CrossRef](#)]
21. Yi, H.A.; Lei, W.A.; Wenju, F.U.; Haitao, Z.H.; Tao, L.I.; Beizhen, X.U.; Ruizhi, C.H. LEO navigation augmentation constellation design with the multi-objective optimization approaches. *Chin. J. Aeronaut.* **2021**, *34*, 265–278. [[CrossRef](#)]
22. Ma, F.; Zhang, X.; Li, X.; Cheng, J.; Guo, F.; Hu, J.; Pan, L. Hybrid constellation design using a genetic algorithm for a LEO-based navigation augmentation system. *GPS Solut.* **2020**, *24*, 1–14. [[CrossRef](#)]
23. Wang, X.; Zhang, H.; Bai, S.; Yue, Y. Design of agile satellite constellation based on hybrid-resampling particle swarm optimization method. *Acta Astronaut.* **2021**, *178*, 595–605. [[CrossRef](#)]
24. Kak, A.; Akyildiz, I.F. Designing Large-Scale Constellations for the Internet of Space Things with CubeSats. *IEEE Internet Things J.* **2021**, *8*, 1749–1768. [[CrossRef](#)]
25. Ge, H.; Li, B.; Nie, L.; Ge, M.; Schuh, H. LEO constellation optimization for LEO enhanced global navigation satellite system (LeGNSS). *Adv. Sp. Res.* **2020**, *66*, 520–532. [[CrossRef](#)]
26. Ravishankar, C.; Gopal, R.; BenAmmar, N.; Zakaria, G.; Huang, X. Next-generation global satellite system with megaconstellations. *Int. J. Satell. Commun. Netw.* **2021**, *39*, 6–28. [[CrossRef](#)]
27. Khalife, J.; Neinavaie, M.; Kassas, Z.M. Navigation with Differential Carrier Phase Measurements from Megaconstellation LEO Satellites. In *2020 IEEE/ION Position, Location and Navigation Symposium (PLANS)*; IEEE: Piscataway, NJ, USA, 2020; pp. 1393–1404. [[CrossRef](#)]
28. Arnas, D.; Lifson, M.; Linares, R.; Avendaño, M.E. Definition of Low Earth Orbit slotting architectures using 2D lattice flower constellations. *Adv. Sp. Res.* **2021**, *67*, 3696–3711. [[CrossRef](#)]
29. Shen, C.; Qiu, Z.D. GPS system simulation based on MatLab/Simulink. *J. Syst. Simul.* **2006**, *18*, 1843–1857.
30. Kazantsev, V.N.; Reshetnev, M.F.; Kozlov, A.G.; Cheremisin, V.F. Overview and design of the Glonass system. In *Proceedings of the International Conference on Satellite Communications (ICSC'94)*, Moscow, Russia, 18–21 October 1994; pp. 207–216.
31. Leopold, R.J.; Miller, A. The IRIDIUM™ Communications System. *IEEE Potentials* **1993**, *12*, 6–9. [[CrossRef](#)]
32. Lee, S.S. Closed-form solution of repeat ground track orbit design and constellation deployment strategy. *Acta Astronaut.* **2021**, *180*, 588–595. [[CrossRef](#)]
33. Shantha Lakshmi, K.; Senthil Kumar, M.P.; Kavitha, K.V.N. Inter-satellite laser communication system. In *Proceedings of the 2008 International Conference on Computer and Communication Engineering (ICCCE08)*, Kuala Lumpur, Malaysia, 13–15 May 2008; pp. 978–983.
34. Hashim, A.H.; Mahad, F.D.; Idrus, S.M.; Supa'at, A.S.M. Modeling and performance study of inter-satellite optical wireless communication system. In *Proceedings of the 2010 International Conference on Photonics (ICP2010)*, Langkawi, Malaysia, 5–7 July 2010.
35. Avendaño, M.; Arnas, D.; Linares, R.; Lifson, M. Efficient search of optimal Flower Constellations. *Acta Astronaut.* **2021**, *179*, 290–295. [[CrossRef](#)]
36. Lee, S.; Mortari, D. Design of constellations for earth observation with intersatellite links. *J. Guid. Control. Dyn.* **2017**, *40*, 1261–1269. [[CrossRef](#)]
37. Vos, E.; Scherpen, J.M.A.; Van Der Schaft, A.J. Equal distribution of satellite constellations on circular target orbits. *Automatica* **2014**, *50*, 2641–2647. [[CrossRef](#)]
38. Turner, A.E. Constellation design using walker patterns. In *Proceedings of the AIAA/AAS Astrodynamics Specialist Conference and Exhibit*, Monterey, CA, USA, 18 August 2002.
39. Arnas, D.; Casanova, D. Nominal definition of satellite constellations under the Earth gravitational potential. *Celest. Mech. Dyn. Astron.* **2020**, *132*, 19. [[CrossRef](#)]
40. Wertz, J.R.; Larson, W.J. *The Space Mission Analysis and Design Process*; Microcosm: Dordrecht, The Netherlands, 1995.
41. Seidelmann, P.K. Report of the IAU WGAS Sub-group on Issues on Time. *Highlights Astron.* **1995**, *10*, 193–196. [[CrossRef](#)]
42. Han, S.; Gui, Q.; Li, J. Analysis of the connectivity and robustness of inter-satellite links in a constellation. *Sci. China Phys. Mech. Astron.* **2011**, *54*, 991–995. [[CrossRef](#)]
43. Myers, B.R. Graphs, networks, and algorithms. *Proc. IEEE* **2008**, *70*, 781–782. [[CrossRef](#)]
44. Noto, M.; Sato, H. Method for the shortest path search by extended Dijkstra algorithm. In *Proceedings of the IEEE International Conference on Systems, Man and Cybernetics*, Nashville, TN, USA, 8–11 October 2000; Volume 3, pp. 2316–2320.